

M. Russu, N. Jula, G. Marina

ISSUES UPON MATERIAL NON-REVERSIBLE DEFORMATION THROUGH ELECTROMAGNETIC FIELD WITH APPLICATIONS IN AMMUNITION ASSEMBLY

*Military Technical Academy,
B-dul. George Cosbuc, 81-83, Sector 5, Bucuresti, Romania*

1. General considerations

In the process of ammunition assembly, the main operation is the mounting of the shell in its casing; this process highly determines the quality of the final product, not only from the dimensions point of view, but from the ammunition precision also.

From the dimension point of view, large mounting tolerances drive to difficult barrel shell insertion or even shell rejection.

The value and the stability of the coupling force in the process of shell manufacturing are paramount in obtaining optimal pressure inside the weapon. This inner pressure is the most important factor that determines the interior and exterior ballistic of the weapon, thus the precision.

The value of the coupling force obtained through non-reversible deformation in electromagnetic field was determined experimental, by measuring the force necessary to extract the shell from its casing.

Currently, for 14,5x114 mm infantry ammunition, a large range of coupling forces are permitted in the assembly process (150 – 600 kgf).

This large range is due to different particularities of the classic mechanical assembly technologies, which use moving parts, in direct contact with the ammunition.

The non-reversible deformation in electromagnetic field technology drives to an increase of dimension standard and quality (eliminating the discontinuities of the mechanical assembly processes) of the ammunition, as well as to a decrease of the range of the coupling forces needed, hence to an increase of the overall ammunition quality and precision.

2. THEORETICAL ISSUES UPON FORCE DETERMINATION IN ELECTROMAGNETIC FIELD

For calculating the forces in the ammunition assembly process through electromagnetic field, we start from the expressions of the volume density of the electric force \bar{f}_e and the volume density of the magnetic force \bar{f}_m . The determination of above-mentioned forces was made assuming linear conditions and neglecting permanent magnetization and permanent electric polarization.

As well as in the Maxwell-Hertz macroscopic electromagnetic theory, we consider corps with continuous spatial distribution, the mass density γ being a continuous function of point and time:

$$\gamma = \gamma(\bar{r}, t). \quad (1)$$

For non-homogenous medium the electric permittivity ε and magnetic permeability μ are considered point and its subsequent mass density, hence:

$$\varepsilon = \varepsilon(\bar{r}, \gamma), \quad (2)$$

$$\mu = \mu(\bar{r}, \gamma). \quad (3)$$

For the determination of the volume density of the electric force \bar{f}_e and the volume density of the magnetic force \bar{f}_m we use the law of energy conservation for an elementary transformation of the corps system and the electromagnetic field in the volume V, bordered by the surface Σ .

The decrease of the electromagnetic field energy equals the sum of electromagnetic energy transferred in conductors (by electric conduction process) and the developed mechanic energy:

$$-\frac{dW}{dt} = P_j + P_m, \quad (4)$$

Where: W is the electromagnetic field energy, P_j the electric conduction process power, P_m mechanical transformed power.

Based on the theorem of electromagnetic energy and the law of energy transformation in the electric conduction process [1], W and P_j can be written:

$$W = \int_V \left(\frac{\vec{E} \cdot \vec{D}}{2} + \frac{\vec{H} \cdot \vec{B}}{2} \right) dV, \quad (5)$$

$$P_j = \int_V \vec{E} \cdot \vec{J} dV, \quad (6)$$

Where: \vec{E} is the electric field intensity vector, \vec{D} electric induction vector, \vec{H} magnetic field intensity vector, \vec{B} magnetic induction vector, \vec{J} conduction electric current density and dV volume element.

The expression of mechanical power P_m depending on the force density \vec{f} and velocity \vec{v} :

$$P_m = \int_V \vec{f} \cdot \vec{v} \cdot dV. \quad (7)$$

Introducing (5), (6) and (7) in relation (4), we have:

$$-\int_V \frac{\partial}{\partial t} \left(\frac{\vec{E} \cdot \vec{D}}{2} + \frac{\vec{H} \cdot \vec{B}}{2} \right) dV = \int_V \vec{E} \cdot \vec{J} dV + \int_V \vec{f} \cdot \vec{v} dV. \quad (8)$$

For the determination of the volume density of the electric force \vec{f}_e and the volume density of the magnetic force, \vec{f}_m we use the local forms of the electromagnetic induction law and magnetic circuit law, given by [1]:

$$\text{rot } \vec{E} = -\frac{\partial \vec{B}}{\partial t} + \text{rot}(\vec{v} \times \vec{B}), \quad (9)$$

$$\text{rot } \vec{H} = \vec{J} + \frac{\partial \vec{D}}{\partial t} + \rho_v \cdot \vec{v} + \text{rot}(\vec{D} \times \vec{v}), \quad (10)$$

Where ρ_v is the volume density of electrical charge.

The local derivative of volume density of electrical charge is:

$$\begin{aligned} \frac{\partial}{\partial t} \left(\frac{\vec{E} \cdot \vec{D}}{2} \right) &= \frac{\partial}{\partial t} \left(\frac{D^2}{2\varepsilon} \right) = \frac{D^2}{2} \cdot \frac{\partial}{\partial t} \left(\frac{1}{\varepsilon} \right) + \frac{\vec{D}}{\varepsilon} \cdot \frac{\partial \vec{D}}{\partial t} = \\ &= -\frac{1}{2} E^2 \frac{\partial \varepsilon}{\partial t} + \vec{E} \cdot \frac{\partial \vec{D}}{\partial t}. \end{aligned} \quad (11)$$

The local derivative of electric permittivity is obtained by time derivation of function $\varepsilon(\vec{r}, \gamma)$ [2]:

$$\frac{d\varepsilon}{dt} = \frac{\partial \varepsilon}{\partial t} + \frac{\partial \varepsilon}{\partial x} \cdot \frac{dx}{dt} + \frac{\partial \varepsilon}{\partial y} \cdot \frac{dy}{dt} + \frac{\partial \varepsilon}{\partial z} \cdot \frac{\partial z}{\partial t} = \frac{\partial \varepsilon}{\partial t} + \vec{v} \cdot \text{grad } \varepsilon. \quad (12)$$

Thus:

$$\frac{d\varepsilon}{dt} = \frac{\partial \varepsilon}{\partial t} + \vec{v} \cdot \text{grad } \varepsilon. \quad (13)$$

If the time derivative of ε is written by use of mass density, we have:

$$\frac{d\varepsilon}{dt} = \frac{d\varepsilon}{d\gamma} \cdot \frac{d\gamma}{dt}. \quad (14)$$

Replacing (14) in (13), we have:

$$\frac{\partial \varepsilon}{\partial t} = \frac{d\varepsilon}{d\gamma} \cdot \frac{d\gamma}{dt} - \vec{v} \cdot \text{grad } \varepsilon. \quad (15)$$

Considering the definition of substantial derivative of volume integral of a scalar field $\alpha(\vec{r}, t)$ [1, 2]:

$$\frac{d}{dt} \int_{V_\Sigma} \alpha dV = \int_{V_\Sigma} \left[\frac{\partial \alpha}{\partial t} + \text{div}(\alpha \cdot \bar{v}) \right] dV, \quad (16)$$

We will obtain the following relation:

$$\begin{aligned} \frac{d\varepsilon}{dt} &= \frac{\partial \varepsilon}{\partial t} + \bar{v} \cdot \text{grad} \varepsilon = \frac{\partial \varepsilon}{\partial t} + \bar{v} \text{grad} \varepsilon + \varepsilon \text{div} \bar{v} - \varepsilon \text{div} \bar{v} = \\ &= \frac{\partial \varepsilon}{\partial t} + \text{div}(\bar{v} \cdot \varepsilon) - \varepsilon \text{div} \bar{v}. \end{aligned} \quad (17)$$

Hence, the mass density derivative can be expressed similar to (17):

$$\frac{d\gamma}{dt} = \frac{\partial \gamma}{\partial t} + \text{div}(\bar{v} \cdot \gamma) - \gamma \cdot \text{div} \bar{v}. \quad (18)$$

Through non-reversible deformation through electromagnetic field technological process, the part suffers a geometric modification; their mass remaining unchanged.

If we consider mass written as:

$$m = \int_V \gamma dV = \text{constant},$$

Thus, based on the mass conservation law, the substantial derivative of the volume integral for the mass density is zero. Further on, based on (16), we have:

$$\frac{\partial \gamma}{\partial t} + \text{div}(\bar{v} \gamma) = 0. \quad (19)$$

Replacing (18) and (19) in (15), we have:

$$\frac{\partial \varepsilon}{\partial t} = -\frac{d\varepsilon}{d\gamma} \cdot \gamma \cdot \text{div} \bar{v} - \bar{v} \cdot \text{grad} \varepsilon. \quad (20)$$

Introducing (20) in (11), we will have the electric energy volume density:

$$\frac{\partial}{\partial t} \left(\frac{\bar{E} \cdot \bar{D}}{2} \right) = \frac{1}{2} \cdot E^2 \cdot \frac{d\varepsilon}{d\gamma} \cdot \gamma \cdot \text{div} \bar{v} + \frac{1}{2} E^2 \bar{v} \text{grad} \varepsilon + \bar{E} \cdot \frac{\partial \bar{D}}{\partial t}, \quad (21)$$

Or:

$$\begin{aligned} \frac{\partial}{\partial t} \left(\frac{\bar{E} \cdot \bar{D}}{2} \right) &= \frac{1}{2} \cdot \text{div} \left(E^2 \cdot \frac{d\varepsilon}{d\gamma} \cdot \gamma \cdot \bar{v} \right) - \frac{1}{2} \cdot \bar{v} \cdot \text{grad} \left(E^2 \cdot \frac{d\varepsilon}{d\gamma} \cdot \gamma \right) + \\ &+ \frac{1}{2} \cdot \bar{v} \cdot E^2 \cdot \text{grad} \varepsilon + \bar{E} \cdot \frac{\partial \bar{D}}{\partial t}. \end{aligned} \quad (22)$$

Using the same algorithm for the magnetic field, described by vectors \bar{B} and \bar{H} we obtain the local derivative for the volume density of the magnetic energy:

$$\begin{aligned} \frac{\partial}{\partial t} \left(\frac{\bar{H} \cdot \bar{B}}{2} \right) &= \frac{1}{2} \text{div} \left(H^2 \frac{d\mu}{d\gamma} \cdot \gamma \cdot \bar{v} \right) - \frac{1}{2} \bar{v} \text{grad} \left(H^2 \frac{d\mu}{d\gamma} \cdot \gamma \right) + \\ &+ \frac{1}{2} \bar{v} H^2 \text{grad} \mu + \bar{H} \cdot \frac{\partial \bar{B}}{\partial t}. \end{aligned} \quad (23)$$

Further on, we calculate the first term on the right of the above relation, for the power equation (8); the mentioned term represents the conductive electric process power.

In the power density relation $\bar{E} \cdot \bar{J}$ the last term (conductive current density) is substituted from relation (10) and the result is:

$$\bar{E} \cdot \bar{J} = \bar{E} \cdot \text{rot} \bar{H} - \bar{E} \cdot \frac{\partial \bar{D}}{\partial t} - \bar{v} \cdot \rho_v \cdot \bar{E} - \bar{E} \cdot \text{rot}(\bar{D} \times \bar{v}). \quad (24)$$

After several iterations for the terms of (24), we obtain [3] the following:

$$\bar{E} \cdot \text{rot} \bar{H} = \text{div}(\bar{H} \times \bar{E}) + \bar{H} \cdot \text{rot} \bar{E}. \quad (25)$$

Moreover, taking into account (9) we have:

$$\bar{E} \cdot \text{rot} \bar{H} = \text{div}(\bar{H} \times \bar{E}) - \bar{H} \cdot \frac{\partial \bar{B}}{\partial t} - \bar{H} \cdot \text{rot}(\bar{B} \times \bar{v}). \quad (26)$$

From the last term of (26) we have:

$$\begin{aligned}\bar{H} \cdot \text{rot}(\bar{B} \times \bar{v}) &= \text{div}\left[(\bar{B} \times \bar{v}) \times \bar{H}\right] + (\bar{B} \times \bar{v}) \times \text{rot}\bar{H} = \\ &= \text{div}\left[(\bar{B} \times \bar{v}) \times \bar{H}\right] - \bar{v}(\bar{B} \times \text{rot}\bar{H}).\end{aligned}\quad (27)$$

Taking the same steps for the last term of (24), we have:

$$\bar{E} \cdot \text{rot}(\bar{D} \times \bar{v}) = \text{div}\left[(\bar{D} \times \bar{v}) \times \bar{E}\right] - \bar{v}(\bar{D} \times \text{rot}\bar{E}).\quad (28)$$

Introducing (26), (27) and (28) in relation (24), we have:

$$\begin{aligned}\bar{E} \cdot \bar{J} &= \text{div}(\bar{H} \times \bar{E}) - \bar{H} \cdot \frac{\partial \bar{B}}{\partial t} - \text{div}\left[(\bar{B} \times \bar{v}) \times \bar{H}\right] + \bar{v}(\bar{B} \times \text{rot}\bar{H}) - \\ &- \bar{E} \cdot \frac{\partial \bar{D}}{\partial t} - \bar{v} \cdot \rho_v \bar{E} - \text{div}\left[(\bar{D} \times \bar{v}) \times \bar{E}\right] + \bar{v}(\bar{D} \times \text{rot}\bar{E}).\end{aligned}\quad (29)$$

Based on (22), (23) and (29) the relation (8) we have the expression of the mechanical transformed power:

$$\begin{aligned}P_m &= \int_V \bar{f} \cdot \bar{v} dV = - \int_V \left\{ \frac{1}{2} \bar{v} \cdot E^2 \text{grad}\varepsilon - \frac{1}{2} \bar{v} \text{grad}\left(E^2 \frac{d\varepsilon}{d\gamma} \cdot \gamma\right) + \bar{E} \cdot \frac{\partial \bar{D}}{\partial t} + \right. \\ &+ \frac{1}{2} \bar{v} \cdot H^2 \text{grad}\mu - \frac{1}{2} \bar{v} \text{grad}\left(H^2 \frac{d\mu}{d\gamma} \cdot \gamma\right) + \bar{H} \cdot \frac{\partial \bar{B}}{\partial t} - \\ &- \bar{H} \cdot \frac{\partial \bar{B}}{\partial t} + \bar{v}(\bar{B} \times \text{rot}\bar{H}) - \bar{E} \cdot \frac{\partial \bar{D}}{\partial t} - \bar{v} \cdot \rho_v \bar{E} + \bar{v}(\bar{D} \times \text{rot}\bar{E}) \left. \right\} dV - \\ &- \int_{\Sigma} \left\{ \frac{1}{2} E^2 \frac{d\varepsilon}{d\gamma} \cdot \gamma \cdot \bar{v} + \frac{1}{2} \cdot H^2 \frac{d\mu}{d\gamma} \cdot \gamma \cdot \bar{v} - \bar{H} \times \bar{E} - (\bar{B} \times \bar{v}) \times \bar{H} - (\bar{D} \times \bar{v}) \times \bar{E} \right\} d\bar{A}.\end{aligned}\quad (30)$$

Where Σ is the bordering surface of V , and $d\bar{A}$ is the surface element of Σ .

The integral on surface Σ from (30) was obtained from the terms for which the divergence from (22), (23) and (29) was calculated through Gauss-Ostrogradski theorem.

If in (30) we separate the two additive terms that represent \bar{f}_e and \bar{f}_m , thus:

$$\bar{f}_e = \rho_v \cdot \bar{E} - \frac{1}{2} \cdot E^2 \text{grad}\varepsilon + \frac{1}{2} \text{grad}\left(E^2 \frac{d\varepsilon}{d\gamma} \cdot \gamma\right) - \bar{D} \times \text{rot}\bar{E}.\quad (31)$$

And

$$\bar{f}_m = -\frac{1}{2} H^2 \text{grad}\mu + \frac{1}{2} \text{grad}\left(H^2 \frac{d\mu}{d\gamma} \cdot \gamma\right) - \bar{B} \times \text{rot}\bar{H}.\quad (32)$$

The terms in relation (31) and (32) represent various action forms of the electromagnetic field towards corpus: $\rho_v \cdot \bar{E}$ - The density of the force exercised towards the volume element of the electrical charged corpus (where the volume density of the electric charge is ρ_v), situated in the field \bar{E} ; $\frac{1}{2} E^2 \text{grad}\varepsilon$ - The density of the force determined by the non-homogenous electric permittivity of the corpus; $\frac{1}{2} H^2 \text{grad}\mu$ - The density of the force determined by the non-homogenous electric permeability of the corpus; $\frac{1}{2} \text{grad}\left(E^2 \frac{d\varepsilon}{d\gamma} \cdot \gamma\right)$ - The density of the electric friction force determined by the variation of electric permittivity function of the corpus density; $\frac{1}{2} \text{grad}\left(H^2 \frac{d\mu}{d\gamma} \cdot \gamma\right)$ - The density of the magnetic friction force determined by the variation of magnetic permeability function of the corpus density.

Due to the fact that almost all shell casing (all ammunition types) are metal-based or metal made, the only term that counts in (31) and (32) is the magnetic one - the magnetic force density.

If in (32) we take in consideration the local form of the electromagnetic induction from (10), in the particular case of zero velocity $\bar{v} = \bar{0}$, (the situation of ammunition assembly process), than, the magnetic force density is:

$$\bar{f}_m = \bar{J} \cdot \bar{B} + \frac{\partial \bar{D}}{\partial t} \times \bar{B} - \frac{1}{2} H^2 \text{grad} \mu + \frac{1}{2} \text{grad} \left(H^2 \frac{d\mu}{d\gamma} \cdot \gamma \right). \quad (33)$$

The magnetic force density has to be regarded as an equivalent density, the experimental observable factor being the total force that interacts towards the corpus:

$$\bar{F} = \int_{V_c} \bar{f}_m \cdot dV. \quad (34)$$

Where V_c represents the corpus volume.

The actual determination of force \bar{F} , based on (34) requests the knowledge of the variation mode of the electric current intensity within the discharging circuit and of the electric induction.

3. THE BLOCK DIAGRAM OF THE ELECTROMAGNETIC FIELD NON-REVERSIBLE DEFORMATION EQUIPMENT

The block diagram of the electromagnetic field non-reversible deformation equipment is depicted by fig. 1.

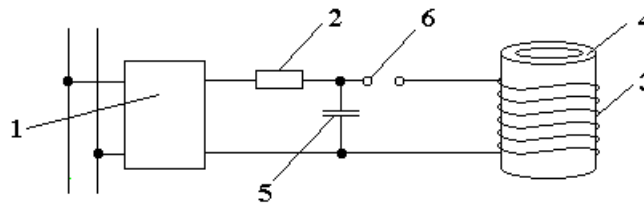


Fig. 1. The block diagram of the electromagnetic field non-reversible deformation equipment.

The notations in figure 1 are:

1 – electrical power source, 2 – resistor, 3 – inductance with the magnetic field concentrator, 4 – subject part, 5 – condenser battery, 6 – breaker.

The magnetic field concentrator provides high values of magnetic field in the deformation area. The role of these components is emphasized by the inductance-concentrator assembly – fig. 2.

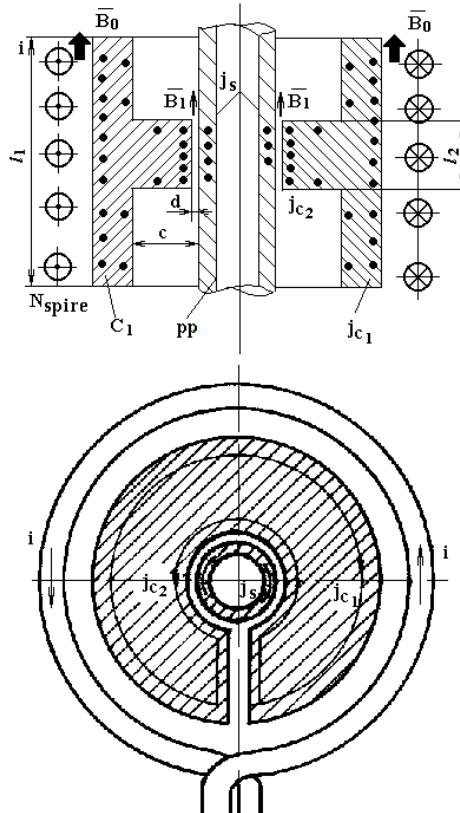


Fig. 2. The inductance and the field concentrator.

Figure 2,a presents a section through the inductance and the field concentrator, and figure 2,b presents the upper view of the assembly.

The discharge of the condenser battery on the inductance (that is made of N spire traveled by the current $i(t)$) an axial time variable magnetic field $B_0(t)$ is produced. The high frequency magnetic field $B_0(t)$ enters the concentrator C_t and determines the apparition of a superficial linear current density J_{C_1} in opposite direction with the inductance current.

Due to the slot that interrupts the field concentrator continuity, the J_{C_1} density current cannot close through this area, thus it will be forced to close through the inner surface of the concentrator, especially in the boundary zone, where it will generate the current density J_{C_2} .

Due to the inner smaller height l_2 (compared to the outer height l_1), the inner current density J_{C_2} will be greater than the outer current density J_{C_1} .

Thus, the magnetic induction at the part surface (in the non-reversible deformation area) increases, hence $B_1 > B_0$. The time variable magnetic induction $B_1(t)$ drives to superficial distributed circular currents of density J_s . The determination of the magnetic field spectrum in the concentrator area can be performed using the complex representation and the Schwartz-Cristoffel method [1, 4].

The basic materials used for field concentrator manufacture have to have low electric resistance and high mechanic stiffness, thus some special alloys will be used: Cu-Be, Cu-Mb or Cu-Cr.

For the determination of electric current intensity within the discharging circuit, we use the equivalent schematic of the circuit, as shown in fig. 3.

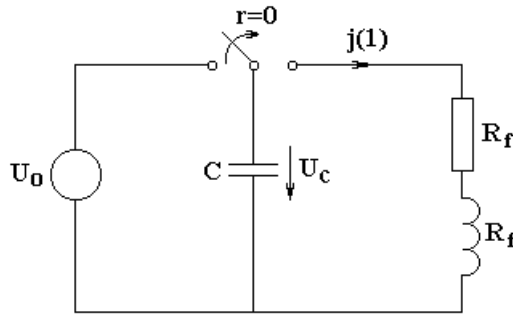


Fig. 3. The equivalent schematic of the discharging circuit.

Where: R_c, L_c concentrator reported resistance and inductance, R_e, L_e equivalent resistance and inductance of the current ways, condenser battery and switching devices.

The condenser C , charged by voltage U_0 from the power supply is coupled at $t=0$ on the discharging circuit. The resistance and inductance of the serial circuit are R_t and L_t , and can be written:

$$R_t = R_c + R_e; \quad L_t = L_c + L_e. \quad (35)$$

The current intensity $i(t)$ in the transient regime through the discharging circuit will be determined by solving the circuit equations:

$$L_t \frac{di}{dt} + R_t i - u_c = 0, \quad (36)$$

$$i = -C \frac{du_c}{dt}. \quad (37)$$

Eliminating in (36) and (37) the term $i(t)$ we obtain a second order differential equation:

$$L_t \cdot C \frac{d^2 U_c}{dt^2} + R_t \cdot C \frac{dU_c}{dt} + U_c = 0. \quad (38)$$

With the general solution:

$$U_c(t) = A e^{p_1 t} + B \cdot e^{p_2 t}. \quad (39)$$

The parameters p_1 and p_2 are the characteristic equation roots:

$$L_t \cdot C p^2 + R_t C p + 1 = 0, \quad (40)$$

Thus:

$$p_{1,2} = -\delta \pm \beta \text{ Where } \delta = \frac{R_t}{2L_t} \text{ and } \beta = \pm \sqrt{\left(\frac{R_t}{2L_t}\right)^2 - \frac{1}{L_t C}}. \quad (41)$$

The constants A and B from (39) are to be determined from initial conditions, based on switching laws [5, 6].

$$i(0_+) = i(0_-) = 0, \quad (42)$$

$$U_c(0_+) = U_c(0_-) = U_0. \quad (43)$$

Hence, we obtain the condenser voltage:

$$U_c(t) = U_0 e^{-\delta t} \left(\text{ch}\beta t + \frac{\delta}{\beta} \text{sh}\beta t \right). \quad (44)$$

The following relation gives the current intensity in the discharging circuit:

$$i(t) = \frac{U_0}{\beta L_t} \cdot e^{-\delta t} \text{sh}\beta t, \quad (45)$$

For which, depending on the discharging circuit parameters we can have various regimes:

a. Non-periodic regime, for $R_t > \sqrt{\frac{L_t}{C}}$, when the function $i(t)$ is given analytical by (45) and is graphical represented in fig. 4.a.

b. The non-periodic critical regime for $R_t = 2\sqrt{\frac{L_t}{C}}$. In this case $\beta = 0$ and the current $i(t)$ is:

$$i(t) = \lim_{\beta \rightarrow 0} \frac{U_0}{\beta L_t} \cdot e^{-\delta t} \text{sh}\beta t = \frac{U_0}{L_t} \cdot t \cdot e^{-\delta t}. \quad (46)$$

The time variation of the current for non-periodic regime is presented in fig. 4b.

c. The damped oscillating regime, for $R_t < 2\sqrt{\frac{L_t}{C}}$.

In this case, we make the following notations:

$$\beta = j\omega; \quad \omega = \omega_0 \sqrt{1 - \left(\frac{R_t}{2\sqrt{\frac{L_t}{C}}}\right)^2}; \quad \omega_0 = \frac{1}{\sqrt{L_t \cdot C}}, \quad (47)$$

Resulting for the current $i(t)$ the analytical expression:

$$i(t) = \frac{U_0}{\omega L_t} \cdot e^{-\delta t} \sin \omega t, \quad (48)$$

Whom graphical representation is shown in fig. 4.c.

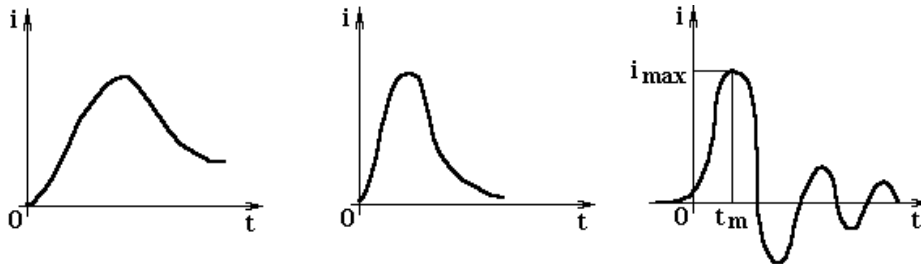


Fig. 4. Variation modes of the discharging current.

From the above described regimes a , b and c , the last is interesting from the electromagnetic field ammunition assembly point-of-view.

The maximum of the first current alternation t_m , is obtained from the condition:

$$\frac{di}{dt} = 0. \quad (49)$$

Hence:

$$-\delta \cdot e^{-\delta t} \sin \omega t + \omega e^{-\delta t} \cos \omega t = 0, \quad (50)$$

Solving the equation with respect to time, we have:

$$t_m = \frac{1}{\omega} \operatorname{arctg} \left(\frac{\omega}{\delta} \right). \quad (51)$$

The corresponding maximum value of the current intensity is obtained by substituting time t_m given by (51) in relation (48) and resulting:

$$I_{\max} = \frac{U_0}{L_t \sqrt{\omega^2 + \delta^2}} \cdot e^{-\delta t_m}. \quad (52)$$

The oscillating current within the installation is in the range of tens of kHz. The energetic efficiency of the installation varies in the range of 10–40, decreasing with the material resistance growth. Generally, the materials able to sustain deformation through this method have to have at least 10% of the Cu electrical conductivity [7].

The installation for electromagnetic field non-reversible deformation works at a low power factor in the range of 0,1–0,6; due to the rectifier module, the installation produces a large harmonic spectrum in the power supply circuits [8], thus the need of taking limiting measures against the mentioned unwanted phenomenon.

4. EXPERIMENTAL DATA AND RESULTS

The experimental data were gathered on the actual assembly process of the infantry 14,5x114 mm ammunition, mounted by use of non-reversible deformation in electromagnetic field. The geometry of the shell is depicted by figure 5.

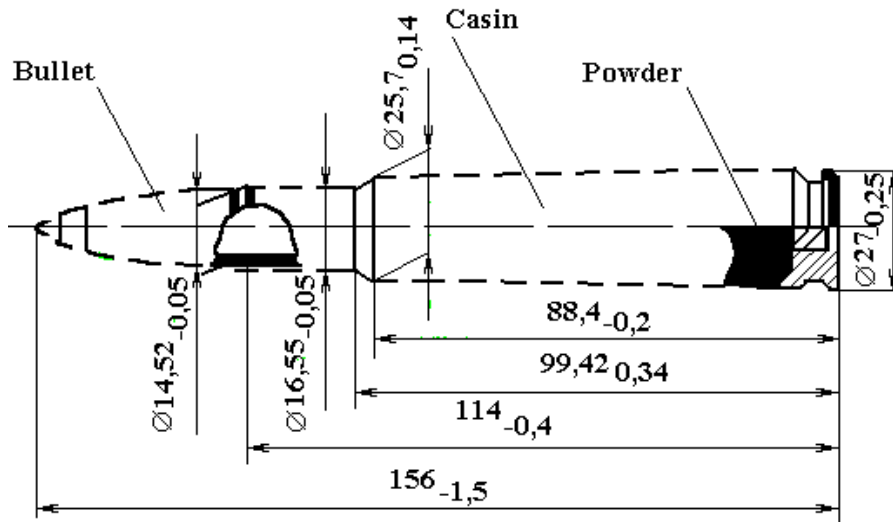


Fig. 5. The geometry of the 14,5x114 mm caliber ammunition.

The assembly process for the above ammunition consists in:

- Forced insertion of an external diameter $\phi=14,92$ mm bullet in the casing with an inner diameter of $\Phi = 14,88$ mm and a tube thickness of 0,7 mm on a length of 14,88 mm.
- The applying of an assembly pressure in the scope of bending the casing collar.

The power source of the experimental installation was chosen to provide $U_0 = 4500V$. As a quality control, procedure a whole batch of ammunition assembled through the electromagnetic process was put to pressure tests, in the goal to determine the critical shell extraction disassembly force.

The extraction force applied to the shell was increased gradually, the experimental results, including the dimensional control being depicted in table.

Probe no.	Extraction force value [kgf]	Dimensional control result
1	165	Admitted
2	256	Admitted
3	305	Admitted
4	324	Admitted
5	316	Admitted
6	319	Admitted
7	305	Admitted
8	290	Admitted
9	278	Admitted
10	253	Admitted

The dimensional control had a checklist of three items: total length of assembled ammunition, width and uniformity of deformed contour, concentricity of ammunition component axis.

The entire ammunition batch passed the test with no rejection.

Analyzing the results from table 1, we can emphasize that using this process, the extraction force needed has a lower dispersion, in the 165–324 kgf range (compared to the mechanical classic process, where the necessary force varies in the 150–600 kgf range).

The result of the above-mentioned lower range drives to a higher accuracy of the batch, when the other firing factors are constant.

5. CONCLUSIONS

The electromagnetic non-reversible assembly process drives to higher quality ammunition.

Initially used in the aerospace industry to assemble high-stiffness materials, the process can be extended to high-resistance ammunition manufacturing.

With no contact between the active elements and the subject part, the last preserve all performance and quality.

The pressure value used within the process can be monitored and controlled in real-time, with high accuracy and precision.

The principle and design of the installation are suitable for integration into an automated/robotic assembly line.

BIBLIOGRAPHY

1. *Mocanu C.I.* Teoria câmpului electromagnetic. Editura Didactică și Pedagogică, București, 1981.
2. *Șabac Gh. I.* Matematici speciale. Vol. 1. Editura Didactică și Pedagogică, București, 1964.
3. *Preda M., Cristea P.* Bazele electrotehnicii. Editura Didactică și Pedagogică, București 1969.
4. *Fluerașu C.* Studiul unui concentrator de câmp pentru formarea electromagnetică. Studii și cercetări în energetică și electrotehnică. Tom. 21. Nr. 1. 1971. Pag. 145–165. București.
5. *Răduleț R.* Bazele electrotehnicii. Problema II. Editura Didactică și Pedagogică. București, 1981.
6. *Gavrilă Gh.* Bazele electrotehnicii. Teoria circuitelor electrice. Vol. II. Editura Academiei Tehnice Militare. 1991. București.
7. *Popescu M., Popescu C.* Tehnologii electrice speciale. Electrotehnologii. Litografia Institutului Politehnic București. 1988.
8. *Șora I., Golovanov N.* Electrotermie și Electrotehnologii. Vol. II, Electrotehnologii. Editura Tehnică. București, 1999.

Received 04.03.02

Summary

The paper presents some theoretical and practical issues upon the non-reversible material deformation technology through electromagnetic field used in the process of shell-to-cartridge assembly in the ammunition manufacture technology. For the non-reversible material deformation technology through electromagnetic field some mathematical and theoretical considerations and demonstrations are presented, as well as interpretations upon the described phenomena. Further on, the basic block schematics for the non-reversible deformation equipment and the magnetic field concentrator are presented, followed by the experimental results obtained from the assembly process of the infantry 14,5×114 mm ammunition.